

Contact Angle Study on Polymer-Grafted Silicon Wafers

Ron S. Faibish,² Wayne Yoshida, and Yoram Cohen¹

Department of Chemical Engineering, University of California—Los Angeles, Los Angeles, California 90095-1592

Received July 16, 2002

Surface wettability and hydrophilicity of terminally grafted PVP and PVAc on smooth silicon wafers were investigated by advancing and receding contact angle measurements. Surface wetting trends correlated with polymer graft yield. Contact angle hysteresis results did not reveal a clear dependence of surface wetting on surface roughness (determined by atomic force microscopy) at the nanoscale level. Surface roughness appeared decrease with increasing chain length for the present surfaces produced by free radical graft polymerization. Contact angle analysis in terms of surface tension components demonstrated that the degree of hydrophilicity of polymer-grafted smooth inorganic surfaces depends on both polymer functionality and polymer graft yield. It is postulated that reorientation of surface-grafted polymer chains could account for changes in surface wettability, similar to those observed for solid polymer films. © 2002 Elsevier Science (USA)

Key Words: surface roughness; contact angle; grafted polymers; surface wettability.

1. INTRODUCTION

In recent years there has been a growing interest in modifying surface properties of inorganic oxides, polymer films, and other solid substrates with tethered polymers. Applications of such surfaces include, colloid stabilization (1–3), adhesion promotion or reduction (4), wetting (5), lubrication (6), biocompatibility (7), size exclusion chromatography (8), and reducing fouling of ultrafiltration membranes (9, 10). In all of the above applications, information regarding surface hydrophilicity (or water wettability) is essential to assessing surface behavior. Contact angle analysis of liquids on native and polymer-modified inorganic and polymeric surfaces has been a preferred, simple, and routinely applied approach to evaluating solid surface free energy, surface tension, and surface wetting characteristics (11, 12). Information obtained from contact angle measurements, for a wide range of solid substrates (e.g., polymer surfaces, ceramics, glass, etc.), has proved vital to the formulation of adhesives, composites, and biocompatible materials and in generating fundamental understanding of solid–solid and solid–liquid intermolecular interactions (e.g., van-der Waals, acid/base type interactions, and electrostatic interactions) (12–18). Despite the

popularity of contact angle analysis, variability in reported measurements is often linked to different contact angle measurement techniques and substrate preparation (11, 19–21). Therefore, great care must be exercised when comparing values obtained from different studies.

For ideal surfaces, which are considered to be rigid, smooth (i.e., surface roughness $\ll 0.5 \mu\text{m}$), and chemically homogeneous (11–13), there exists only one contact angle, which is the true equilibrium contact angle. However, for real surfaces (rough, heterogeneous, and/or nonrigid), there may be several observed contact angles, which results in contact angle hysteresis (22). Thus, the advancing/receding contact angle measurement method, which quantifies hysteresis, is especially suited for assessing the impact of surface chemistry and topology on surface wettability of polymer-modified surfaces, which are the focus of the present study.

In the present work, advancing and receding contact angle measurements with three different fluids were obtained to investigate surface wettability and estimate surface free energy of tethered hydrophilic polymer poly(vinyl pyrrolidone) [PVP] and a hydrophobic polymer poly(vinyl acetate) [PVAc] formed by graft polymerization of their building-block monomers onto smooth silicon wafer surfaces. Surface topology images and surface roughness of the native and polymer-grafted silicon wafers were obtained from atomic force microscopy (AFM) analysis. Surface wettability and surface free energy trends for the different polymer-modified surface were assessed using polar and apolar surface tension components as well as contact angle hysteresis analysis.

2. ANALYSIS

Surface tension components of polymer-grafted silicon wafers were determined from contact angle measurements using the method outlined by van Oss (13) with polar and apolar liquids. These components were then used to evaluate wettability, hydrophilicity, and contact angle hysteresis behavior of the PVP- and PVAc-grafted wafer surfaces. A summary of the above approach is provided in the proceeding sections, and the interested reader is referred elsewhere (13, 23–29) for additional details.

2.1. Polar and Apolar Surface Energy Components

The fundamental equation which relates the interfacial tension between solid and liquid (γ_{SL}) to solid surface tension (γ_{S}), liquid

¹ To whom correspondence should be addressed. Fax: (310) 206-4107. E-mail: yoram@ucla.edu.

² Current address: International Atomic Energy Agency, Vienna, Austria.

surface tension (γ_L), and the contact angle (θ) between a drop of liquid and a chemically homogeneous, nonadsorbing, smooth, and horizontal (i.e., ideal) solid surface, is given by the well-known Young's equation (23):

$$\gamma_{SL} = \gamma_S - \gamma_L \cos \theta \quad (\theta > 0). \quad [1]$$

The various surface tension components in Young's equation can be subdivided into apolar (γ^{LW} , accounting for the Lifshitz-van der Waals type interactions) and polar (γ^{AB} , accounting for acid-base or electron donor-acceptor type interactions) subcomponents according to (13, 24, 25)

$$\gamma_i = \gamma_i^{LW} + \gamma_i^{AB}, \quad [2]$$

where the subscript i denotes S, L, or SL. The polar component, γ^{AB} , can be further subdivided by using specific terms for an electron donor (γ^-) and an electron acceptor (γ^+) subcomponents (26):

$$\gamma_i^{AB} \equiv 2\sqrt{\gamma_i^+ \gamma_i^-}. \quad [3]$$

According to the theory presented by van Oss and Good (25), apolar and polar components of the interfacial liquid/solid tension are given by

$$\gamma_{SL}^{LW} = (\sqrt{\gamma_S^{LW}} - \sqrt{\gamma_L^{LW}})^2 \quad [4a]$$

and

$$\gamma_{SL}^{AB} = 2(\sqrt{\gamma_S^+} - \sqrt{\gamma_L^+})(\sqrt{\gamma_S^-} - \sqrt{\gamma_L^-}). \quad [4b]$$

The combination of Eqs. [1]–[4] results in a modified form of the Young–Dupre equation,

$$(1 + \cos \theta)\gamma_L^T = 2(\sqrt{\gamma_S^{LW}\gamma_L^{LW}} + \sqrt{\gamma_S^+\gamma_L^-} + \sqrt{\gamma_S^-\gamma_L^+}), \quad [5]$$

where γ_L^T is the total surface energy (per unit area) of the liquid. The three solid surface tension components (γ_S^{LW} , γ_S^- , γ_S^+) can be determined by solving three simultaneous equations in the form of Eq. [5] using known surface tension components of two polar solvents and one apolar solvent (13). Common solvents used for such an analysis include water (polar), glycerol (polar), formamide (polar), α -bromonaphthalene (apolar), and diiodomethane (apolar). Once the three solid tension components are determined, the total surface tension of the solid, γ_S^T , can be determined from

$$\gamma_S^T = \gamma_S^{LW} + 2\sqrt{\gamma_S^+\gamma_S^-}. \quad [6]$$

It is noted that substances for which $\gamma^- \ll \gamma^+$ or $\gamma^+ \ll \gamma^-$ are considered to be monopolar (13, 25). For these substances, the total surface tension is essentially equal to γ^{LW} (see Eqs. [2] and

[3]). In order to determine whether a substance is predominantly monopolar, a typical practice is to compare the values of its γ^- or γ^+ components to those of water (i.e., a reference substance with $\gamma^- = \gamma^+ = 25.5 \text{ mJ/m}^2$). This is accomplished by evaluating the polarity ratios (13),

$$\delta_{iW}^- = \sqrt{\gamma_i^- / \gamma_W^-} \quad [7a]$$

or

$$\delta_{iW}^+ = \sqrt{\gamma_i^+ / \gamma_W^+} \quad [7b]$$

where δ_{iW}^- and δ_{iW}^+ are the relative Lewis acid and Lewis base polarities, respectively, of substance i with respect to water. A substance i is considered to be a γ^+ monopole (i.e., exclusively electron-acceptor) if $\delta_{iW}^- \ll 0.2$ and a γ^- monopole (i.e., exclusively electron donor) if $\delta_{iW}^+ \ll 0.2$ (13). Monopolar substances can exhibit strong interactions with materials of opposite polarity, despite the seemingly apolar nature of their surface tension (i.e., $\gamma_i = \gamma^A$). The hydrophilic or "hydrophobic" nature of a substance can also be evaluated via knowledge of the substance polarity and the free energy of hydration (i.e., the interaction free energy between a substance and water), ΔG_{iW} , which is obtained from the Young–Dupre equation (13),

$$\Delta G_{iW} = \gamma_{iW}^T - \gamma_i^T - \gamma_W^T = -\gamma_W^T(1 + \cos \theta_W) \quad [8]$$

in which γ_i^T is the total surface tension of substance i , γ_W^T is the total surface tension of water (both given by equations similar to Eq. [6]), θ_W is the contact angle a water sessile drop makes with the solid surface, and γ_{iW}^T is the total interfacial tension between substance i and water given by (13, 25)

$$\begin{aligned} \gamma_{iW}^T &= \gamma_{iW}^{LW} + \gamma_{iW}^{AB} = (\sqrt{\gamma_i^{LW}} - \sqrt{\gamma_W^{LW}})^2 \\ &\quad + 2(\sqrt{\gamma_i^+} - \sqrt{\gamma_W^+})(\sqrt{\gamma_i^-} - \sqrt{\gamma_W^-}) \end{aligned} \quad [9]$$

The relative magnitude of γ_i^- for different substances (particularly polymeric substances) can be considered to be roughly proportional to the hydrophilicity of substance i (13). It has been argued that a measure of the autophilicity (self-attraction) of a substance, when this substance is in a water medium, provides additional insight to the concept of hydrophilicity. The above measure is described by ΔG_{iWi} , the free energy change in bringing substance i , immersed in water (W), from infinity to a minimum equilibrium distance in which a very thin layer of water separates two macroscopic bodies of substance i . This free energy is given by

$$\Delta G_{iWi} = -2\gamma_{iW}. \quad [10]$$

It has been shown that ΔG_{iWi} correlates with the interaction free energy between a substance and water (i.e., free energy

of hydration) ΔG_{iW} (13). Experimental observations for a large set of compounds reveal that when $\Delta G_{iWi} > 0$, $\Delta G_{iW} < -113 \text{ mJ/m}^2$; in other words, substance i can be considered more hydrophilic. When $\Delta G_{iW} > -113 \text{ mJ/m}^2$ (i.e., $\Delta G_{iWi} < 0$) substance i should be considered more “hydrophobic” (13). The word “hydrophobic” is put in quotation marks since even apolar compounds can attract water to a considerable degree. (ΔG_{iW} ranges from about -40 mJ/m^2 for the majority of apolar substances (e.g., hexane, $\Delta G_{iW} = -40.0 \text{ mJ/m}^2$) to under -140 mJ/m^2 for most polar substances (e.g., poly(ethylene oxide) [PEO], $\Delta G_{iW} = -142.0 \text{ mJ/m}^2$) (13). Thus, as argued by van Oss (13) it is more appropriate to state that a substance is more or less hydrophilic (or less or more autophilic when in contact with water) than to claim that it is more or less hydrophobic. Notwithstanding, the term “hydrophobic,” which has been entrenched in the scientific literature, is also adopted in the present study. It is also apparent that there is no absolute scale for the degree of hydrophilicity of various substances; thus, the free energy of hydration should always be regarded as a relative measure of hydrophilicity when comparing different substances.

2.2. Contact Angle Hysteresis

Contact angle hysteresis, H , exists when there is inequality of the advancing angle θ_a and receding angle θ_r (see section 3):

$$H \equiv \theta_a - \theta_r. \quad [11]$$

It has been shown that the advancing contact angle is less sensitive to surface roughness and heterogeneity than the receding angle. Therefore, advancing angle data are commonly used to calculate surface and interfacial tension components (27–29). Contact angle hysteresis has been attributed to solid surface roughness, surface chemical heterogeneity, swelling, penetration of liquid into the solid surface, and surface reorientation of functional groups (11, 24, 30–35, and refs. therein). Surface roughness is not expected to result in contact angle hysteresis for surfaces with rugosities less than approximately $0.5 \mu\text{m}$ (i.e., smooth surfaces) (11). On the other hand, a number of studies (24, 30–35) have reported that surface chemical heterogeneities, surface swelling, penetration of liquid into the solid surface, and surface reorientation of chemical functional groups can all lead to contact angle hysteresis, even on smooth surfaces.

3. EXPERIMENTAL

3.1. Materials

Silicon $\langle 100 \rangle$ wafers of 100 mm in diameter and 0.050–0.055 mm in thickness were obtained from Wafernet, Inc. (San Jose, CA). Nonporous silica particles (Novacite L207-A) of about $5 \mu\text{m}$ in diameter and surface area of $2.2 \text{ m}^2/\text{g}$ were supplied by Malvern Minerals Co. (Hot Springs, AR). Formamide [FA] (superpure grade), diiodomethane [DIM] (laboratory grade), 30% hydrogen peroxide (certified, ACS), concentrated H_2SO_4 , concentrated HCl, KOH pellets, xylenes, ethyl

acetate, vinyl acetate, and methanol (certified, ACS) were obtained from Fisher Scientific (Pittsburgh, PA). Ultrapure deionized (DI) water was obtained by treating distilled water through a Milli-Q Water System (Millipore Corp., San Jose, CA). Trimethoxyvinylsilane and vinylpyrrolidone were purchased from Aldrich Chemicals (Milwaukee, WI), and 2,2'-azobis(2,4-dimethylpentanenitrile) [Vazo 52] was purchased from Dupont (Wilmington, DE).

3.2. Pretreatment of Silicon Wafers and Silica Particles

Native silicon wafers were cleaned, prior to modification, by overnight immersion in a 7 : 3 volume ratio mixture of 30% H_2O_2 and concentrated H_2SO_4 , followed by a thorough rinse with DI water and oven drying under vacuum overnight at 110°C . The naturally mined Novacite silica particles, which served as surrogate surfaces for determining polymer graft yield, were pretreated by the recommended method (36) consisting of dispersing the particles in a 2% concentrated HCl solution for 3 h followed by rinsing with DI water and oven drying under vacuum overnight at 110°C .

3.3. Surface Modification of Silicon Wafers and Silica Particles

Silicon wafers and silica particles were modified via an established two-step reaction with intermediate treatment steps (36–38, 40). Details of the reaction mechanism and kinetics of the graft polymerization reaction can be found elsewhere (36–41). In the first step (i.e., surface activation), vinyltrimethoxysilane (VTMS) was covalently bonded to silanol groups on the particles and wafers surfaces. The resulting surface-bonded vinyl groups served as the anchoring sites for polymer chains that were grafted to the surface via free-radical graft polymerization (Fig. 1). Silylation of the wafers or particles with VTMS was carried out for a period of 5 h in a VTMS solution in xylene maintained at just below the boiling point of xylene ($\approx 134^\circ\text{C}$). The silylated substrate was thoroughly rinsed with xylene and oven-dried overnight under vacuum at a temperature of 140°C .

The details of the experimental methods can be found elsewhere for vinyl acetate (37, 39) and vinylpyrrolidone (36–38) graft polymerization. Briefly, the silylated wafers or particles were used without further treatment for graft polymerization of vinylacetate (VA) using 2,2'-azobis(2,4-dimethylpentanenitrile) [Vazo 52] as the initiator. However, prior to graft polymerization of vinylpyrrolidone (VP), in an aqueous medium, the particles or wafers were hydrolyzed using KOH to convert unreacted surface methoxy groups to silanols, thereby improving the wettability of the substrate surface. The graft polymerization reactions were carried out for a period of about 6–8 h under the reaction conditions listed in Table 1. At the termination of the reaction, the polymer-modified substrates were thoroughly washed with DI water (for PVP) or ethyl acetate (for PVAc) to remove nongrafted PVP or PVAc chains. The polymer-modified surfaces consisted of polyvinylacetate and polyvinylpyrrolidone chains terminally

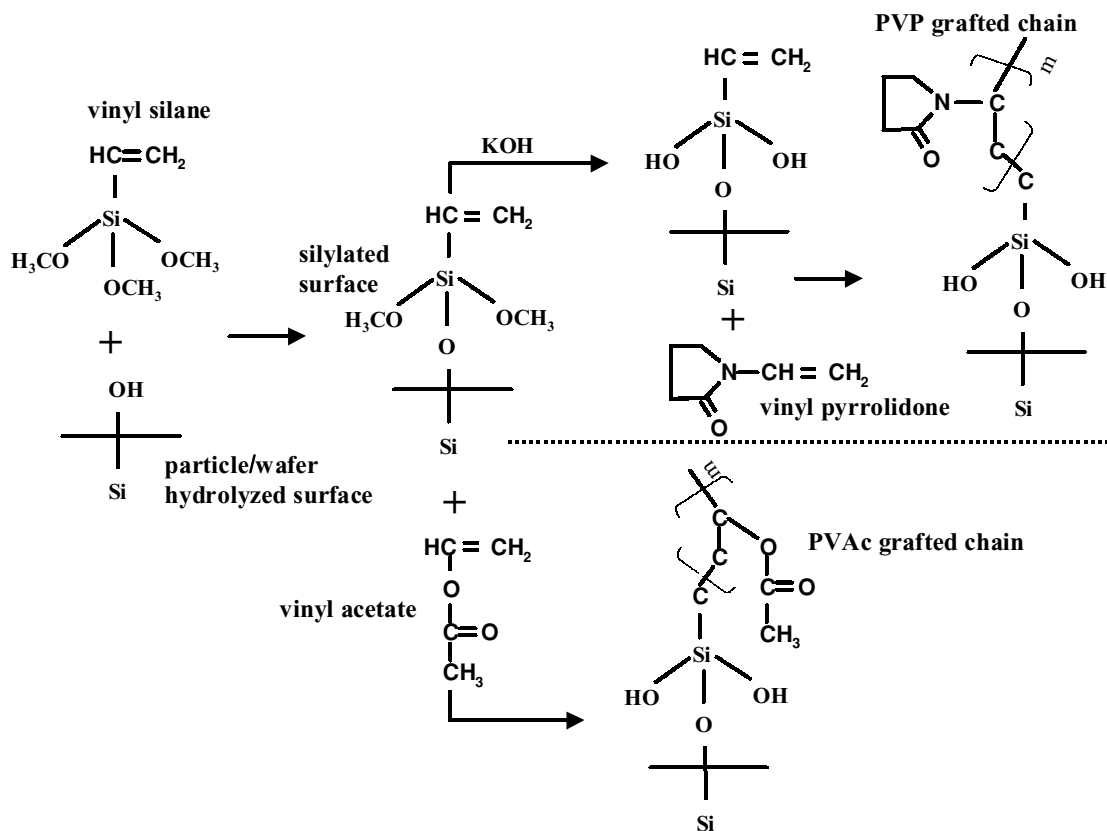


FIG. 1. Surface modification reactions. In the first step, the surface is silylated with vinyl silanes. In the second step, PVP (above the dashed line) is grafted after the silylated surface is hydrolyzed (to yield a more hydrophilic surface), while PVAc is grafted without VTMS hydrolysis.

anchored to the inorganic substrate (see Fig. 1). Polymer graft yield for the grafted silica particles (expressed on an area basis, mg/m²) was determined by thermogravimetric analysis (TGA) using a TGA TGS-2 system (Perkin-Elmer, Norwalk, CT).

3.4. Contact Angle Measurements

Advancing and receding contact angle measurements for three different liquids (DI water, formamide, and diiodomethane)

were performed following the sessile drop method (24) with a Kruss Model G-23 (Hamburg, Germany) contact angle instrument. Each reported contact angle measurement represents an average value of at least four separate drops on different areas of a given wafer. The size and volume of the drops were kept constant (within a fraction of a mm) since it is known that variations in the volume of the drops can lead to inconsistent contact angle measurements (20, 32, 33). Final contact angle measurements were recorded (usually within 10–15 s) once their values

TABLE 1
Grafting Reaction Conditions and Properties of Polymer-Grafted Substrates for PVP and PVAc

Grafting conditions	Initial monomer concentration (vol %)	Reaction temperature (°C)	Graft yield ^a (mg/m ²)	\bar{M}_n (kDa)	Chain spacing, <i>D</i> (nm)	<i>R</i> _{RMS} (nm)
PVP ^b	M10T70	10	70	1.27	7.00	3.55
	M30T70	30	70	1.52	13.6	0.82
	M30T80	30	80	2.63	12.2	1.14
PVAc ^c	M10T60	10	60	0.80	18.8	3.89
	M40T50	40	50	2.52	47.3	3.32
	M40T60	40	60	3.54	39.7	3.62
Native wafer						0.21

^a Based on polymer-grafted surrogate silica particles (36, 38, 40).

^b Reaction initiator, H₂O₂, concentration = 0.043 M; NH₄OH (cocatalyst and buffer) concentration = 0.030 M.

^c Reaction initiator, Vazo 52, concentration = 0.030 M.

did not change after drop placement. The above approach was followed to minimize transient droplet shape variations due to droplet relaxation and spreading. Prior to each set of contact angle measurements the wafers were cleaned by ethanol and water rinses according to the following sequence: three rinses with ethanol, two with water, one with ethanol, and three with water. The wafers were subsequently oven-dried under vacuum for 10 min at 120°C and immediately placed in sealed containers (17). Measurements were conducted at a constant relative humidity of 65% and temperature of 21.5°C. Repeat measurements of a given contact angle were all within $\pm 2^\circ$.

3.5. Atomic Force Microscopy (AFM) Imaging

The surface topology of the native and polymer-modified wafers was imaged using a Digital Instruments (Santa Barbara, CA) multimode atomic force microscope with a Nanoscope IIIa SPM controller, operating in tapping mode. All images were taken for dry surfaces under air atmosphere. In order to ascertain the presence of image artifacts trace and retrace AFM scans (where the trace and retrace scans are from left to right and right to left, respectively) were compared during the scan of the polymer grafted surfaces. The images were essentially identical for both the trace and retrace scans. In addition, a 90° rotation of the scan direction was also carried out verifying the absence of any directionally dependent features or artifacts. Images were also found to be essentially identical after multiple scans, demonstrating that scans did not damage the surface or alter the surface topology.

All 3-D images of the wafer surfaces were obtained from $1 \times 1\text{-}\mu\text{m}$ wafer regions. Average surface root-mean-square roughness (R_{RMS}) values were obtained from analysis of 4 to 7 different $5 \times 5\text{-}\mu\text{m}$ areas on each wafer. The R_{RMS} values were calculated from

$$R_{\text{RMS}} = \sqrt{\frac{\sum_{n=1}^N (z_n - \bar{z})^2}{N - 1}}, \quad [12]$$

where z_n is the height of a random location on the scanned surface, \bar{z} is the mean height of all measured heights, and N is the sample size (i.e., number of height values).

4. RESULTS AND DISCUSSION

4.1. Summary of Surface Grafting and AFM Results

The polymer graft yield for PVP and PVAc ranged from 0.76 to 2.9 mg/m² (Table 1). Molecular weight data for PVP grafted onto surrogate silica particles, for the present range of reaction conditions, were available in the literature (38, 40) (Table 1). However, similar data are unavailable for PVAc-grafted surfaces, primarily due to the difficulty in degrafting of PVAc for molecular weight analysis. Notwithstanding, one can estimate the molecular weight of grafted PVAc given that the size of these chains

should be similar to the formed homopolymer chains (within about $\pm 10\%$ (38)). Accordingly, the number-average molecular weight of the grafted PVP and PVAc chains (Table 1), formed at the present reaction conditions, is estimated to range from about 7×10^3 – 1.4×10^3 and 1.9×10^4 – 10^4 g/mol, respectively (38, 40–42). For the present range of reaction conditions, the polydispersity index (i.e., \bar{M}_w/\bar{M}_n) ranged from about 2 to 5 (36, 40), and the grafted chain spacing was in the range of 2.9–6.2 nm (Table 1). AFM images of the polymer-modified surfaces reveal a heterogeneous surface topology (Fig. 2) that is consistent with the fact that the polymer chains, formed by free-radical polymerization, are polydisperse (36–38, 40). While there are obvious variations in grafted surface roughness for the different polymer grafted surfaces, AFM images at nanoscale resolution suggest that the surfaces are fully populated with polymer chains.

Surface roughness (Eq. [13]) of the polymer-modified wafers was significantly higher relative to the native wafer (Table 1 and Fig. 2). The native wafer was smooth with a root-mean-square (RMS) roughness of only 0.21 nm, which was smaller by a factor of ~ 4 – 18 than the roughness of the polymer-grafted wafers (Table 1). The above observations should be regarded with caution since both polymer-modified surfaces consist of polydisperse chains. Available data for PVP grafted surfaces indicates that the grafted chain polydispersity for the M10T70, M30T70, and M30T80 surfaces (4.9, 2.8, and 3.1, respectively) correlates with surface roughness. This behavior could be the result of smaller chains providing less drastic elevation drops from the higher surface features. Clearly, more focused topological study is warranted to explore the above hypothesis.

4.2. Contact Angle Results and Analysis

4.2.1. Wafer wetting characteristics. The native wafer was by far the most wetting toward the hydrophilic water and formamide solvents as was evident from the low water contact angles and contact angle hysteresis ($\theta_a = 11$; $\theta_r = 6$; $H = 5$). We note that similar water contact angles were reported on a smooth glass plate which was cleaned with chromic acid prior to contact angle measurements ($\theta_a = 12$ and $\theta_r = 10$) (43). The low water contact angles on the native wafer surface are indicative of a hydrolyzed, clean and smooth wafer surface prior to modification. In contrast, a marked increase in the contact angle was measured for the polymer-grafted surfaces (Table 2), even for the water-soluble PVP chains. This behavior is likely to be associated with the hydrophobic backbone of the polymer chains.

The wettability of the polymer-grafted surface can be examined by comparing the contact angles for water and diiodomethane (DIM) since these two solvents are often used as reference liquids in analyses of the interactions of polar and apolar solvents with solid surfaces. An examination of the advancing water contact angle, θ_a , which is often regarded as the angle closest in value to the equilibrium contact angle of the low-energy component of the contaminated or composite material (27–29), reveals that θ_a decreased (by 47%) with increasing polymer graft

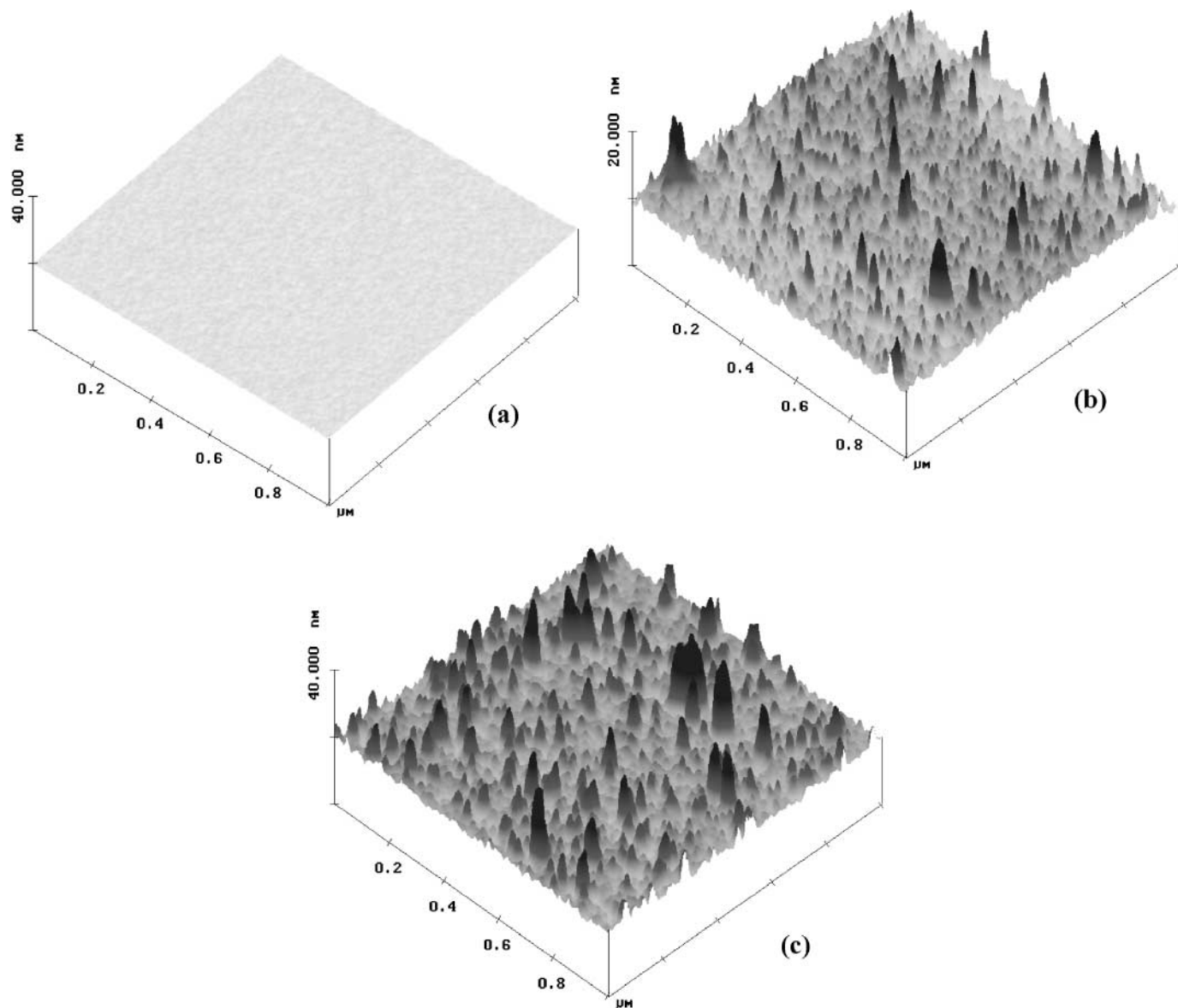


FIG. 2. Tapping mode AFM images of (a) native wafer, (b) PVP M30T70 grafted wafer, and (c) PVAc M40T60 grafted wafer.

yield (from 1.27 to 2.63 mg/m²) for the PVP-grafted wafers (Table 2a). For the PVAc-grafted wafers, θ_a increased (by 14%) as the graft yield increased from 0.80 to 3.54 mg/m² (see Table 2b). On the other hand, θ_a for DIM, on the same surfaces, decreased (by 40%), over the experimental range of graft yields, for the PVAc-grafted surfaces; in contrast, θ_a remained essentially constant for the PVP-grafted surfaces. The decrease in θ_a for water on the PVP-grafted wafers and DIM on the PVAc-grafted wafers is attributed, in part, to the increase in polymer graft yield on the wafer surface and consequently greater surface wetting by either water (a good solvent for the PVP-grafted surfaces) or DIM (a good solvent for the PVAc-grafted surfaces). It is plausible that the decrease in water contact angle for the M10T70 relative to the M30T70 wafers was primarily

due to the longer grafted PVP chain size, despite the greater chain spacing, which exposes the more hydrophobic silylated substrate (Tables 2a and 1, respectively). However, greater wettability (i.e., lower water contact angle) of the M30T80 wafer, compared to that of the M30T70 wafer, is more likely due to an increase in polymer graft yield and the lower chain spacing (or higher grafted chain density by about 24%). This latter result can be rationalized by considering the estimated volume fraction of the tethered polymer chains, within the grafted polymer surface layer, ϕ_P , when exposed to water (i.e., good solvent for PVP) as (44)

$$\phi_P \cong \frac{Na\sigma}{L_c}, \quad [13]$$

TABLE 2

Advancing Angle (θ_a), Receding Angle (θ_r), and Contact Angle Hysteresis ($H = \theta_a - \theta_r$) for (a) PVP- and (b) PVAc-Grafted Silicon Wafers

Grafting conditions	Graft yield (mg/m ²)	Water		Formamide		Diiodomethane	
		θ_a/θ_r	H	θ_a/θ_r	H	θ_a/θ_r	H
(a) PVP							
M10T70	1.27	72/27	45	57/32	25	46/34	12
M30T70	1.52	57/21	36	34/20	14	48/30	18
M30T80	2.63	38/17	21	24/16	8	47/27	20
(b) PVAc							
M10T60	0.80	64/34	30	61/25	36	55/32	23
M40T50	2.52	69/28	41	50/25	25	43/27	16
M40T60	3.54	73/24	49	52/24	28	33/19	14

where a is the monomer size [nm], N is the degree of polymerization, σ is the fractional surface coverage ($\sigma = (a/D)^2$, where D is the chain spacing [nm]). The average chain extension can be estimated (40) as $L_c = Na\sigma^{1/3}$ [nm]. The monomer sizes, determined using the molecular simulation package Hyperchem 6.0, were approximately 4.3 Å for PVAc and 6.4 Å for PVP. Since ϕ_p was found to be higher for the M30T80 wafer than for the M30T70 wafer ($\phi_p = 0.071$ and 0.050, respectively), water sorption capacity (i.e., wettability) should be expected to be higher for the M30T80 wafer.

Previous studies (14, 15, 45, 46) have shown that the static water contact angle (determined by the sessile drop method) generally decreases for “hydrophobic” polymer surfaces (e.g., polyethylene and poly(ethylene terephthalate)) grafted with hydrophilic polymers (e.g., acrylamide and acrylic acid) as the grafting reaction time and/or initial monomer concentration, both of which lead to an increase in the mass of grafted polymer, are increased. Unfortunately, the above studies did not provide information regarding surface heterogeneities and roughness associated with polymer grafting. It is interesting to note, however, that in a more recent study, Fadeev and McCarthy (17) suggested that a greater surface coverage of silicon wafers with “hydrophobic” trialkylsilane was responsible for the observed increase in the advancing water contact angle. In another study, Drellich *et al.* (47) demonstrated that the receding and advancing contact angles can reach a maximum with respect to the surface density of chemisorbed unsaturated carboxylic acids.

In the present study, further characterization of surface wettability was performed by calculating surface tension components (or surface free energy; see section 2.1) using contact angle measurements for three different fluids whose surface tensions component data are given in Table 3. The analysis revealed that reduction of water contact angle for the PVP-grafted wafers, with increasing PVP graft yield, was accompanied by an increase in the γ^- surface polar subcomponent (Table 4a). Similarly, the contact angle decrease for DIM on the PVAc-grafted surfaces corresponds to a decrease in γ^- and to an increase in γ^{LW} , i.e., to stronger Lifshitz–van der Waals interactions (Table 4b). This

TABLE 3

Solvent Surface Tension Components at 20°C (mJ/m²)^a

Liquid	γ^{LW}	γ^+	γ^-	γ^{AB}	γ^T
Water	21.8	25.5	25.5	51.0	72.8
Formamide	39.0	2.28	39.6	19.0	58.0
Diiodomethane (DIM)	50.8	~0	0	0	50.8

^a Source: van Oss (13).

implies that polar (i.e., electron-donor/electron acceptor) interactions become stronger as the more hydrophilic PVP chains are grafted onto the wafer surface and become weaker as the more hydrophobic PVAc chains are grafted onto the wafers. The slight increase in the water advancing contact angle on the PVAc-grafted wafers, with increasing graft yield (Table 2b), is consistent with previous studies of water contact angle behavior on polymer surfaces with electron-rich functional groups (31, 43). In these latter studies it was argued that both hydrophilic and “hydrophobic” surface polymer chains can favorably interact with water through reorientation of polar (typically electron-rich) functional groups toward the top surface in contact with water (31, 46). Polar group reorientation could be especially important for polymers with asymmetric repeating units (46), such as PVAc and PVP (see Fig. 1). Such surface chain reorientation could also contribute to contact angle hysteresis, as discussed in section 4.2.2, below. Clearly, it would be useful in future studies to confirm surface chain orientation through appropriate spectroscopic techniques such as ATR-FTIR surface analysis.

4.2.2. Contact angle hysteresis. Contact angle hysteresis was encountered for all of the polymer-modified wafer surfaces for both good and poor solvents (Table 2). Contact angle hysteresis decreased (by as much as 53%) with increasing graft yield for good solvents (water for the PVP-grafted wafers and DIM for and PVAc-grafted wafers) (Fig. 3). In addition, as polymer graft yield increased, the grafted polymer surface became more wetting toward the good solvent. Thus, both receding and advancing angles, and consequently contact angle hysteresis, decreased (Table 2). It is interesting to note that,

TABLE 4

Surface Tension Components and Free Energy of Hydration for (a) PVP- and (b) PVAc-Grafted Silicon Wafers (all Units in mJ/m²)

Grafting conditions	γ^{LW}	γ^+	γ^-	γ^{AB}	γ^T	δ^-/δ^+
(a) PVP						
M10T70	36.3	0.1	13.1	2.3	38.6	0.72/0.06
M30T70	35.4	2.3	16.8	12.4	47.8	0.81/0.30
M30T80	35.8	2.2	34.2	17.3	51.5	1.16/0.29
(b) PVAc						
M10T60	31.4	0	26.8	0	31.4	1.03/0
M40T50	38.0	0.3	12.8	3.9	41.9	0.50/0.11
M40T60	43.0	0.1	9.2	1.9	44.9	0.60/0.06

while the advancing contact angle for DIM (hydrophobic poor solvent for PVP) on the PVP-grafted wafers was nearly invariant, the receding angle *decreased* (Table 2a). It is plausible that the present seemingly anomalous result is due to reorientation of the hydrophilic functional groups of the PVP chains *away* from the top surface which is in contact with the DIM drop (see section 4.2.1). As a result, the less hydrophilic hydrocarbon PVP backbone (see Fig. 1) is exposed and wetted by DIM. This reasoning is further supported by a similar trend of a decrease in the receding water (hydrophilic poor solvent for PVAc) contact angle on the PVAc-grafted surfaces (Table 2a). In this latter case, the electron-donating monopolar character of the PVAc-grafted surfaces ($\delta^+ < 0.2$, see Table 4b), which is due to the presence and reorientation of the electron-rich ester functional group of PVAc (see section 4.2.1), enhances the attraction between the receding water molecules and grafted polymer chains resulting in a decreasing receding contact angle with increasing polymer graft yield (Tables 1 and 2b).

Although the present results reveal a variation in surface roughness with grafting conditions, a correlation between contact angle hysteresis and surface roughness (on the order of

nanometers) was not apparent (Fig. 3). Indeed, previous studies, have suggested that contact angle hysteresis should not be affected by surface roughness below $\sim 0.5 \mu\text{m}$ when surface roughness is considered (11–13, 28, 49 and refs. therein). We note that a few studies (17, 47) did attribute contact angle hysteresis to molecular scale surface roughness; however, no definitive quantitative correlations with surface roughness or quantitative assessment of the contribution of other possible factors have been reported (e.g., surface heterogeneity).

4.2.3. Surface hydrophilicity. The relative surface hydrophilicity for the different polymer-modified surfaces can be evaluated by examining the free energy hydration, ΔG_{iW} (see section 2.1). Accordingly, as can be seen from Fig. 4, two of the three PVAc-grafted wafers (M10T60 and M40T50) can be considered more hydrophilic than the least hydrophilic PVP-grafted wafer (M10T70). Therefore, the strict classification of the PVAc-grafted surfaces as “hydrophobic” in nature, due to the low solubility of PVAc in water (only 3–6% by mass water uptake) (50), may be misleading, as is the expectation that all the PVP-grafted wafers would exhibit the same degree of hydrophilicity.

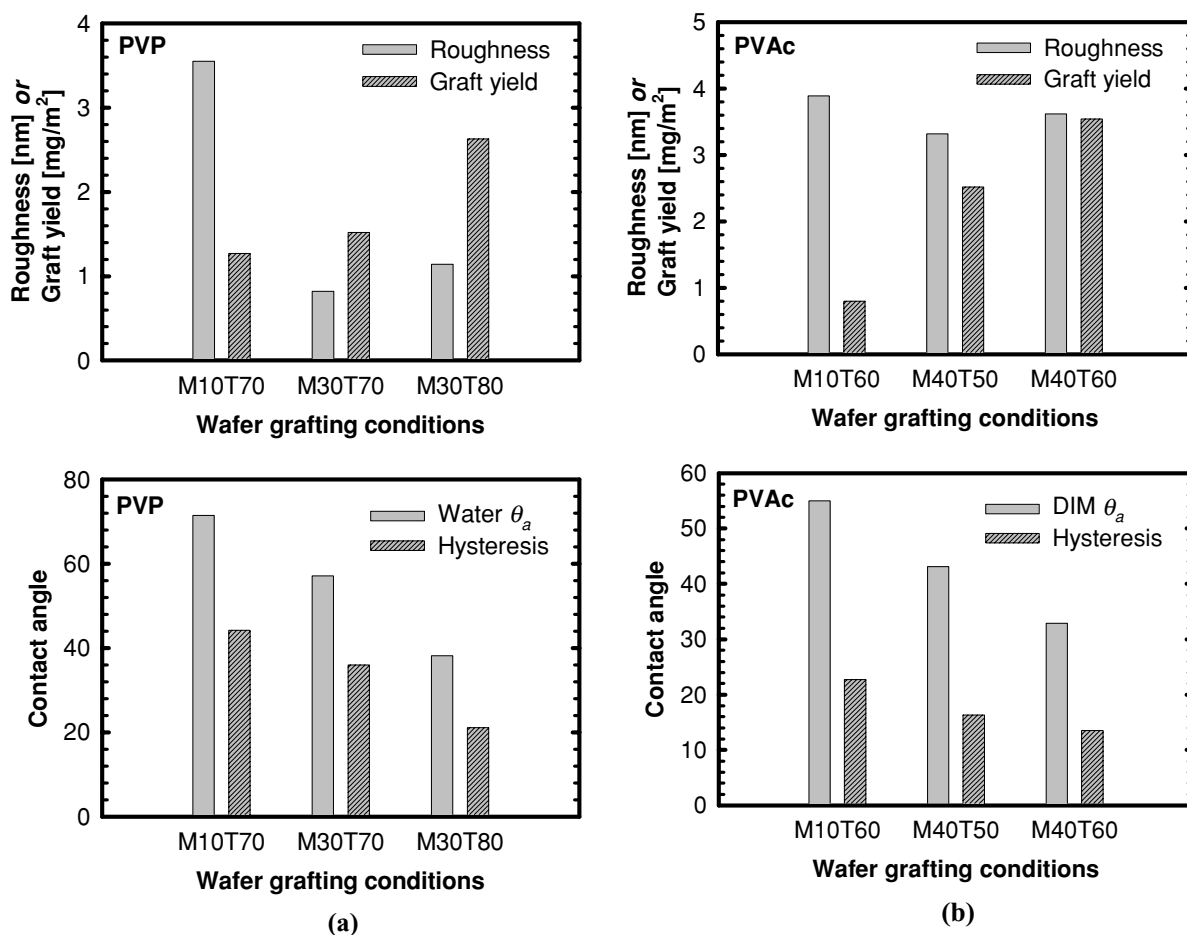


FIG. 3. Trends in graft yield, surface roughness (R_{RMS}), advancing contact angle (θ_a), and contact angle hysteresis ($H = \theta_a - \theta_r$) for the (a) PVP- and (b) PVAc-grafted wafers for different reaction conditions.

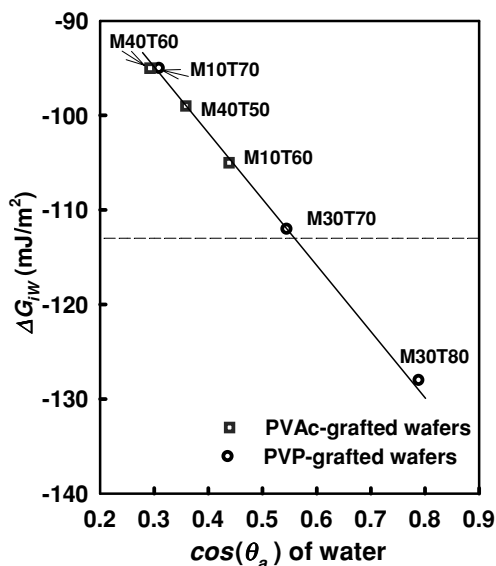


FIG. 4. Relative hydrophilicity of PVP- and PVAc-grafted wafers as determined from the relation between surface wettability and surface free energy of hydration (ΔG_{iw}).

It is also apparent that the only truly hydrophilic polymer-grafted surface, according to the definition in section 2.1, is the PVP-grafted wafer with the highest polymer graft yield (M30T80) for which $\Delta G_{iw} < -113 \text{ mJ/m}^2$. As the above analysis suggests, for the range of grafting conditions and the grafting method used in the present study (see Figs. 3 and 4), polymer graft yield is an important factor in rendering polymer-grafted surfaces more or less hydrophilic. The above results suggest the relative degree of surface hydrophilicity as evaluated from contact angle measurements for polymer-grafted surfaces would benefit from consideration of polymer surface coverage.

5. CONCLUSIONS

Surface wettability and hydrophilicity trends for silicon wafer surfaces modified with terminally grafted PVP and PVAc chains was studied via contact angle analysis. For the present range of surface densities (i.e., chain spacing of 2.9–6.2 nm) surface wettability (assessed by advancing and receding contact angle measurements) correlated with polymer chain length and was clearly impacted by the polymer graft yield. Contact angle hysteresis did not appear to correlate with nanoscale surface roughness of tethered polymer surfaces.

Surface wettability was enhanced (i.e., decreasing contact angle of good solvent with the grafted surface) when the electron-donor (γ^-) polar subcomponent of the surface tension (i.e., surface free energy) for the PVP-grafted wafers and the apolar surface tension component (γ^{LW}) and total surface tension (γ^{T}) for the PVAc-grafted wafers increased. It is plausible that the modest increase ($\sim 14\%$) of the water advancing contact angle, with increasing PVAc graft yield, is due, in part, to surface reorientation of the electron-rich functional groups of the PVAc

chains. Polymer chain reorientation could also account for the observed decrease of receding contact angle for diiodomethane [DIM] (a poor solvent for PVP) the PVP-grafted wafers. In the latter case, the decrease in the receding contact angle of the apolar DIM could be attributed to reorientation of the hydrophilic pyrrolidone ring away from the liquid front of the DIM drop. The present study suggests that future studies on the design and characterization of hydrophilic/hydrophobic of tethered polymer surfaces would benefit from considerations of the surface topology and potential surface layer swelling and orientation of surface groups of grafted polymers when exposed to solvents of varying solvation power.

REFERENCES

- Napper, D. H., "Steric Stabilization of Colloidal Dispersions." Academic Press, New York, 1983.
- Gast, A., and Leibler, L., *Macromolecules* **19**, 686 (1986).
- Laible, R., and Hamann, K., *Adv. Colloid Interface Sci.* **13**, 65 (1980).
- Raphael, E., and de Gennes, P. G., *J. Phys. Chem.* **96**, 4002 (1992).
- de Gennes, P. G., *Rev. Mod. Phys.* **57**, 827 (1985).
- Klein, J., *Annu. Rev. Mater. Sci.* **26**, 581 (1996).
- Hair, M., "The Chemistry of Biosurfaces." Dekker, New York, 1971.
- Cohen, Y., Faibish, R. S., and Rovira-Bru, M., in "Interfacial Phenomena in Chromatography" (E. Pefferkorn, Ed.), Vol. 80 of Surfactant Science Series, pp. 263–310. Dekker, New York, 1999.
- Faibish, R. S., and Cohen, Y., *J. Membr. Sci.* **185**, 129 (2001).
- Ulbricht, M., and Belfort, G., *J. Membr. Sci.* **111**, 193 (2001).
- Johnson, R. E., Jr., and Dettre, R. H., in "Surface and Colloid Science" (E. Matijevic, Ed.), Vol. 2, pp. 85–153. Wiley-Interscience, New York, 1969.
- Morra, M., Occhiello, E., and Garbassi, F., *Adv. Colloid Interface Sci.* **32**, 79 (1990).
- van Oss, C. J., "Interfacial Forces in Aqueous Media." Dekker, New York, 1994.
- Yamada, K., Kimura, T., Tsutaya, H., and Hirata, M., *J. Appl. Polym. Sci.* **44**, 993 (1992).
- Yamada, K., Tsutaya, H., Tatekawa, S., and Hirata, M., *J. Appl. Polym. Sci.* **46**, 1065 (1992).
- Brzoska, J. B., Ben Azouz, I., and Rondelez, F., *Langmuir* **10**, 4367 (1994).
- Fadeev, A. Y., and McCarthy, T. J., *Langmuir* **15**, 3759 (1999).
- Schreiber, H. P., *J. Adhesion* **37**, 51 (1992).
- Drelich, J., Miller, J. D., and Good, R. J., *J. Colloid Interface Sci.* **179**, 37 (1996).
- Spelt, J. K., and Vargha-Butler, E. I., in "Applied Surface Thermodynamics" (A. W. Neumann and J. K. Spelt, Eds.), Vol. 63 in Surfactant Science Series, pp. 379–411. Dekker, New York, 1996.
- Blake, T. D., and Haynes, J. M., in "Progress in surface and Membrane Science" (J. F. Danielli, et al., Eds.), pp. 125–138. Academic Press, New York, 1973.
- Dick, J. D., Good, R. J., and Neuman, A. W., *J. Colloid Interface Sci.* **53**, 235 (1975).
- Young, T., *Phil. Trans. R. Soc. London* **95**, 65 (1805).
- Good, R. J., in "Contact Angle, Wettability and Adhesion" (K. L. Mittal, Ed.), pp. 3–36. VSP, 1993.
- van Oss, C. J., and Good, R. J., *J. Macromol. Sci.—Chem.* **A 26**, 1183 (1989).
- van Oss, C. J., Good, R. J., and Chaudhury, M. K., *Langmuir* **4**, 884 (1988).
- Kwok, D. Y., Leung, A., Lam, C. N. C., Li, A., Wu, R., and Neumann, A. W., *J. Colloid Interface Sci.* **206**, 44 (1998).
- Chaudhury, M. K., "Short-Range and Long-Range Forces in Colloidal and Macroscopic Systems," Ph.D. dissertation, SUNY, Buffalo 1984.
- Good, R. J., *Surf. Colloid Sci.* **11**, 1 (1979).

30. Cassie, A. B. D., *Discuss. Faraday Soc.* **3**, 11 (1948).
31. Yasuda, T., and Okuno, T., *Langmuir* **10**, 2435 (1994).
32. Marmur, A., *Adv. Colloid Interface Sci.* **50**, 121 (1994).
33. Marmur, A., *Colloid Surf. A* **136**, 209 (1998).
34. Huh, C., and Mason, S. G., *J. Colloid Interface Sci.* **60**, 11 (1977).
35. Hazlett, R. D., in "Contact Angle, Wettability and Adhesion" (K. L. Mittal, Ed.), pp. 173–181. VSP, 1993.
36. Chaimberg, M., and Cohen, Y., *Ind. Eng. Chem. Res.* **30**, 2534 (1991).
37. Cohen, Y., Yoshida, W., Nguyen, V., Jou, J. D., and Bei, N., in "Oxides Surfaces" (J. A. Wingrave, Ed.). Dekker, New York, 2001.
38. Nguyen, V., Yoshida, W., Jou, J. D., and Cohen, Y., *J. Polym. Sci. A* **40**, 26 (2002).
39. Browne, T., Chaimberg, M., and Cohen, Y., *J. Appl. Polym. Sci.* **44**, 671 (1992).
40. Nguyen, V., Yoshida, W., and Cohen, Y., *J. Appl. Polym. Sci.*, in press.
41. Ito, K., *J. Polym. Sci.* **10**, 1481 (1972).
42. Taylor, T. W., and Reichert, K. H., *J. Appl. Polym. Sci.* **30**, 227 (1985).
43. Tretinnikov, O. N., and Yoshito, I., *Langmuir* **10**, 1606 (1994).
44. de Gennes, P. G., *Macromolecules* **13**, 1069 (1980).
45. Ruckert, D., and Geuskens, G., *Eur. Polym. J.* **32**, 201 (1996).
46. Uchida, E., Uyama, Y., and Ikada, Y., *J. Appl. Polym. Sci.* **41**, 677 (1990).
47. Drelich, J. D., Atia, A. A., Yalamanchili, M. R., and Miler, J. D., *J. Colloid Interface Sci.* **178**, 720 (1996).
48. Miller, J. D., Veeramasuneni, S., Drelich, J., and Yalamanchili, M. R., *Polym. Eng. Sci.* **36**, 1849 (1996).
49. Dettre, R. H., and Johnson, R. E., Jr., *Adv. Chem.* **43**, 136 (1964).
50. Brandrup, J., and Immergut, E. H. (Eds.), "Polymer Handbook." Wiley-Interscience, New York, 1975.